UC Berkeley
UC Berkeley Previously Published Works

Title

PandaX-II constraints on spin-dependent WIMP-nucleon effective interactions

Permalink

Authors

Xia, Jingkai
Abdukerim, Abdusalam
Chen, Wei
et al.

Publication Date

DOI

Peer reviewed

Constraining WIMP-Nucleon Effective Interactions from PandaX-II Experiment

Jingkai Xia,[1] Abdusalam Abdukerim,[2] Xun Chen,[1] Yunhua Chen,[3] Xiangyi Cui,[1] Deqing Fang,[4] Changbo Fu,[1] Karl Giboni,[1] Franco Giuliani,[1] Linhui Gu,[1] Xuyuan Guo,[3] Zhifan Guo,[5] Ke Han,[1] Changda He,[1] Shengming He,[3] Di Huang,[1] Xingtao Huang,[6] Zhou Huang,[1] Peng Ji,[7] Xiangdong Ji,[1,8,*] Yonglin Ju,[5] Shaoli Li,[1] Heng Lin,[1] Huaxuan Liu,[5] Jianglai Liu,[1,8] Yugang Ma,[4] Yajun Mao,[9] Kaixiang Ni,[1] Jinhua Ning,[3] Xiangxiang Ren,[1] Fang Shi,[1] Andi Tan,[10] Anqing Wang,[6] Cheng Wang,[5] Hongwei Wang,[4] Meng Wang,[6] Qiuhong Wang,[4] Siguang Wang,[9] Xiuli Wang,[5] Xuming Wang,[1] Zhou Wang,[5] Mengmeng Wu,[7] Shiyong Wu,[3] Mengjiao Xiao,[10,11] Pengwei Xie,[8] Binbin Yan,[6] Jijun Yang,[1] Yong Yang,[1] Chunxu Yu,[7] Jumin Yuan,[6] Jianfeng Yue,[3] Dan Zhang,[10] Hongguang Zhang,[1] Tao Zhang,[1] Li Zhao,[1] Qibin Zheng,[12] Jifang Zhou,[3] Ning Zhou,[1,†] and Xiaopeng Zhou[9]

(PandaX-II Collaboration)

Wick C. Haxton[13,14,‡]

[1]*INPAC and School of Physics and Astronomy, Shanghai Jiao Tong University,*
Shanghai Key Laboratory for Particle Physics and Cosmology, Shanghai 200240, China
[2]*School of Physics and Technology, Xinjiang University, Ürümqi 830046, China*
[3]*Yalong River Hydropower Development Company,*
Ltd., 288 Shuanglin Road, Chengdu 610051, China
[4]*Shanghai Institute of Applied Physics, Chinese Academy of Sciences, Shanghai 201800, China*
[5]*School of Mechanical Engineering, Shanghai Jiao Tong University, Shanghai 200240, China*
[6]*School of Physics and Key Laboratory of Particle Physics and Particle*
Irradiation (MOE), Shandong University, Jinan 250100, China
[7]*School of Physics, Nankai University, Tianjin 300071, China*
[8]*Tsung-Dao Lee Institute, Shanghai 200240, China*
[9]*School of Physics, Peking University, Beijing 100871,China*
[10]*Department of Physics, University of Maryland, College Park, Maryland 20742, USA*
[11]*Center of High Energy Physics, Peking University, Beijing 100871, China*
[12]*School of Medical Instrument and Food Engineering,*
University of Shanghai for Science and Technology, Shanghai 200093, China
[13]*Department of Physics, University of California, Berkeley, CA 94720, USA*
[14]*Lawrence Berkeley National Laboratory, Berkeley, CA 94720, USA*

(Dated: July 6, 2018)

We present constraints on the WIMP-nucleon effective interaction from the PandaX-II experiment. We consider well-motivated dimensional-four interactions consisting of couplings among vector and axial vector currents, as well as several typical dimension-five and dimension-six operators in effective field theory. The data set corresponding to a total exposure of 54-ton-day is reanalyzed, and limits on the effective couplings have been obtained as a function of the WIMP mass, both in isoscalar and isovector channels. We obtain the most stringent upper limits on spin-dependent WIMP-nucleon cross section of $9.0 \times 10^{-42} \text{cm}^2$ for neutron-only coupling with mass of 40 GeV/c^2 at 90% confidence level. Similarly, the minimum constraint on WIMP-proton cross section is $2.2 \times 10^{-38} \text{cm}^2$.

Astrophysical and cosmological observations indicate that a large amount of non-luminous dark matter (DM) exists in our universe, constituting $\sim 27\%$ of the closure density. However, the exact nature of DM remains a mystery. One intriguing DM candidate, a weakly-interacting massive particle (WIMP), arises naturally in many extensions of the standard model [1, 2]. Many WIMP searches have been performed, including direct detection of their scattering off target nuclei, indirect detection of their decay or annihilation, and their production in collider experiments. In the analysis of direct detection experiments, it has been standard practice to assume the scattering arises from leading-order vector- or axial-vector-mediated interactions, generating spin-independent (SI)

or spin-dependent (SD) WIMP-nucleus scattering, respectively. Constraints on the WIMP-nucleon scattering cross sections σ_p and σ_n have been sharpened by more than an order of magnitude in recent years [3], due to the stringent null results obtained successively in the LUX [4, 5], PandaX [6, 7] and XENON [8–10] experiments.

However, there are other candidate interactions besides the standard SI and SD cases, as has become apparent from effective field theory (EFT) treatments of direct detection. In particular, a nucleon-level EFT employing nonrelativistic, Galilean invariant WIMP-nucleon operators has been developed that includes all interactions through next-to-next-to-leading-order (NNLO) [11]. The

operators are the low-energy equivalents of a corresponding set of relativistic, covariant operators. Thus a given WIMP-nucleon relativistic interaction can be reduced, in general, to a linear combination of the nonrelativistic operators. The fourteen independent non-relativistic operators can be constructed from four linearly independent quantities: the relative perpendicular velocity between the WIMP and the nucleon ($\vec{v}^\perp$), the momentum transfer ($\vec{q}$), and the spins of WIMP and nucleon ($\vec{S}_\chi$, $\vec{S}_N$). Each EFT operator has independent couplings to protons and neutrons, and the framework also allows interference between certain operators. Thus much larger parameter space beyond the standard SI and SD approaches remains to be explored. Previously, direct detection analyses performed by SuperCDMS and XENON100 have deduced additional constraints from generalized EFT analyses [12, 13].

In this paper, we study constraints on a number of WIMP-nucleon EFT interactions from PandaX-II experiment. The experiment, located in the China Jinping Underground Laboratory (CJPL), has recently reported WIMP search results for a total exposure of 54-ton-days [6]. The experiment provided the most stringent upper limit published to date on the SI WIMP-nucleon cross section for WIMP masses larger than 100 GeV/c^2. The lowest 90% C.L. exclusion cross section limit, $8.6 \times 10^{-47}\text{cm}^2$, was obtained at 40 GeV/c^2. PandaX-II is a dual-phase xenon time-projection chamber with 580 kg of liquid xenon in the sensitive target volume. When the incoming WIMP scatters off a xenon nucleus, both the prompt scintillation photons ($S1$) in the liquid and the delayed proportional scintillation photons ($S2$) in the gas are collected by 55 top and 55 bottom Hamamatsu R11410-20 3-inch photomultiplier tubes. We use the 54-ton-day exposure data from PandaX-II experiment to constrain the coupling coefficients for a number of relativistic WIMP-nucleon EFT interactions of current interest [14]. These relativistic EFT interactions can also be probed in high energy collider experiments [15–17].

In the calculations, we assume scattering of spin-1/2 WIMPs on a natural xenon target. We consider here four dimension-four and three higher dimension effective interactions, selected from Table 1 of Ref. [11], defining the operator dimension as 4 + number of powers of m_M in the denominator, where m_M represents mass scale that would in general be determined from a given ultraviolet theory. Four dimension-four effective interactions corresponding to the possible relativistic the vector/axial-vector interactions,

$$\mathcal{L}^5_{\text{int}} \equiv \bar{\chi}\gamma^\mu\chi\bar{N}\gamma_\mu N \rightarrow \mathcal{O}_1$$

$$\mathcal{L}^7_{\text{int}} \equiv \bar{\chi}\gamma^\mu\chi\bar{N}\gamma_\mu\gamma^5 N \rightarrow -2\mathcal{O}_7 + 2\frac{m_N}{m_\chi}\mathcal{O}_9$$

$$\mathcal{L}^{13}_{\text{int}} \equiv \bar{\chi}\gamma^\mu\gamma^5\chi\bar{N}\gamma_\mu N \rightarrow 2\mathcal{O}_8 + 2\mathcal{O}_9$$

$$\mathcal{L}^{15}_{\text{int}} \equiv \bar{\chi}\gamma^\mu\gamma^5\chi\bar{N}\gamma_\mu\gamma^5 N \rightarrow -4\mathcal{O}_4 . \tag{1}$$

The vector-vector interaction $\mathcal{L}^5_{\text{int}}$ reduces to the standard SI interaction in the nonrelativistic limit appropriate in direct detection, while the axial vector-axial vector interaction $\mathcal{L}^{15}_{\text{int}}$ generates the standard SD interaction. In each case a nonrelativistic reduction has been performed to yield results in terms of the Galilean-invariant operators $\mathcal{O}_i$ of Ref. [11]. The operators $\mathcal{O}_1 = 1_\chi 1_N$ and $\mathcal{O}_4 = \vec{S}_\chi \cdot \vec{S}_N$ represent the SI and SD interactions, respectively. Operators $\mathcal{O}_7 = \vec{S}_N \cdot \vec{v}^\perp$ and $\mathcal{O}_8 = \vec{S}_\chi \cdot \vec{v}^\perp$ depend on the WIMP-nucleon relative velocity, while $\mathcal{O}_9 = i(\vec{S}_\chi \times \vec{S}_N) \cdot \vec{q}$ vanishes in the long wavelength limit.

The higher dimension operators we choose to study are the dimension-five operators coupling the WIMP magnetic moment or electric dipole moment with the nucleon's vector current, and the dimension-six operator coupling WIMP and nucleon magnetic moments, given respectively by

$$\mathcal{L}^9_{\text{int}} \equiv \bar{\chi}i\sigma^{\mu\nu}\frac{q_\nu}{m_M}\chi\bar{N}\gamma_\mu N$$

$$\rightarrow -\frac{\vec{q}^2}{2m_\chi m_M}\mathcal{O}_1 + \frac{2m_N}{m_M}\mathcal{O}_5 - \frac{2m_N}{m_M}(\frac{\vec{q}^2}{m_N^2}\mathcal{O}_4 - \mathcal{O}_6)$$

$$\mathcal{L}^{17}_{\text{int}} \equiv i\bar{\chi}i\sigma^{\mu\nu}\frac{q_\nu}{m_M}\gamma^5\chi\bar{N}\gamma_\mu N \rightarrow \frac{2m_N}{m_M}\mathcal{O}_{11}$$

$$\mathcal{L}^{10}_{\text{int}} \equiv \bar{\chi}i\sigma^{\mu\nu}\frac{q_\nu}{m_M}\chi\bar{N}i\sigma_{\mu\alpha}\frac{q^\alpha}{m_M}N \rightarrow 4(\frac{\vec{q}^2}{m_M^2}\mathcal{O}_4 - \frac{m_N^2}{m_M^2}\mathcal{O}_6)$$

$$\tag{2}$$

The electric dipole moment interaction is odd under both parity and time reversal. The operators $\mathcal{O}_5 = i\vec{S}_\chi \cdot (\vec{q} \times \vec{v}^\perp)/m_N$, $\mathcal{O}_6 = (\vec{S}_\chi \cdot \vec{q})(\vec{S}_N \cdot \vec{q})/m_N^2$, and $\mathcal{O}_{11} = i\vec{S}_\chi \cdot \vec{q}/m_N$ have an explicit dependence on $\vec{q}$. Thus the WIMP-nucleus scattering cross sections for the three selected relativistic operators vanish in the long-wavelength limit. Consequently the analysis strategy to constrain such operators can be optimized by weighting events with higher momentum transfer.

The relativistic interaction densities $\mathcal{L}^i_{\text{int}}$ carry coefficients of the form

$$\frac{d^0_i}{m_V^2} + \frac{d^1_i}{m_V^2}\tau_3 = \frac{d^p_i}{m_V^2}\frac{1+\tau_3}{2} + \frac{d^n_i}{m_V^2}\frac{1-\tau_3}{2}$$

where the d_i are dimensionless, defining the strength of the interaction relative to the weak scale

$$m_V \equiv \langle v \rangle = (2G_F)^{-\frac{1}{2}} = 246.2 \text{ GeV}$$

with $\langle v \rangle$ the Higgs vacuum expectation value.

In the numerical work we will describe later, we consider isoscalar ($d^1_i = 0$) and isovector ($d^0_i = 0$) interactions, for which $d^p_i = d^n_i$ and $-d^p_i = d^n_i$, respectively; as

well as couplings only to protons ($d_i^1 = d_i^0$) and only to neutrons ($d_i^1 = -d_i^0$). The choice of isospin coupling is particularly important for spin-dependent scattering off odd-A target nuclei, as the response is effectively governed by whether the unpaired valence nucleon carrying the nuclear spin is a proton or a neutron.

The differential cross section for elastic scattering can be expressed as

$$
\begin{aligned}
\frac{d\sigma(v, E_R)}{dE_R} &= 2m_T \frac{d\sigma(v, \vec{q}^2)}{d\vec{q}^2} \\
&= \frac{2m_T}{4\pi v^2} \left[\frac{1}{2J_\chi + 1} \frac{1}{2J_N + 1} \sum_{\text{spins}} |\mathcal{M}|^2 \right] \quad (3)
\end{aligned}
$$

where the square of the Galilean invariant amplitude $\mathcal{M}$ is a product of WIMP and nuclear matrix elements and is a function of initial WIMP velocity v (dimensionless, in units of c) and the three-momentum transfer $\vec{q}$ [11]. Here J_χ is the WIMP spin and J_N the nuclear ground state angular momentum. In the long wavelength limit the nuclear response functions take relatively simple forms, depending on nuclear matrix elements of familiar operators such as $1(i)$, $\vec{\sigma}(i)$, $\vec{\ell}(i)$, $\vec{\sigma}(i) \cdot \vec{\ell}(i)$, etc. Their relative magnitudes can vary by orders of magnitude. The corresponding differential event rate with respect to the recoil energy is

$$
\frac{dR}{dE_R} = \frac{\rho_\chi}{m_\chi} \int \frac{d\sigma(v, E_R)}{dE_R} v f(\vec{v}) d^3 v, \quad (4)
$$

where the $f(\vec{v})$ is the normalized velocity distribution of the WIMP particles. We calculate WIMP signal rates by evaluating Eq. (4) for a local WIMP mass density of $\rho_\chi = 0.3$ GeV/c^2/cm^3 and assuming a Maxwellian WIMP velocity distribution with the most probable value at $v_0 = 220$ km/s, truncated at the galactic escape velocity $v_{esc} = 544$ km/s.

To translate the experimental results to the constraints on the couplings of different interactions, we need to use theoretical calculations of nuclear matrix elements. We employ full-basis shell-model (SM) calculations using the GCN5082 [18] interaction (so named because the SM valence space resides between the shell closures at nucleon numbers 50 and 82). The basis for ^{129}Xe contains about three billion Slater determinants, while those for the even-A xenon isotopes that play roles in the other response functions we consider below range up to about nine billion Slater determinants. The full GCN5082 response functions are contained in the updated Mathematica script of [19] that we employ. In the case of the SI isoscalar interaction, the use of the Helm form factor is a standard practice [20]. As the form factor is determined by A at $\vec{q}^2 = 0$ and as the slope is effectively governed by the known nuclear radius R, there is little difference between the SM calculation and Helm form factor until one approaches the diffraction minimum of the former appearing at high $\vec{q}^2 \sim 1/R^2$.

For the case of SD couplings, related proton-only or neutron-only chiral EFT matrix elements by Klos *et al.* [21] are available. This calculation also employs the GCN5082 interaction, though with certain basis truncations to reduce the size of the SM space. It includes, in addition to the dominant SD operator $\mathcal{O}_4$, contributions from a pseudoscalar interaction having the form of $\mathcal{O}_6$ of [11] and a pion exchange current, in which the WIMP scatters off a two-nucleon correlation. The odd-A isotopes of xenon would be described naively as a single unpaired neutron residing above of spin-paired core. As this neutron carries the nuclear spin, a strong neutron-coupled SD response is expected. In fact the SD calculations we carried out confirm this naive expectation, finding that the neutron-coupled SD cross section is about three orders of magnitude larger than the corresponding proton-coupled response. Consequently the SD and chiral EFT calculations agree well, with both spin-dominated, despite the more complicated operator structure of the latter and despite some differences in the SM calculations, as described above. However, when the coupling is only to protons, the SD response is highly suppressed by the valence isospin structure, and significant differences appear between the SD and chiral EFT results.

In Fig. 1 we give the recoil energy spectra in SM calculations for the four vector-axial vector spectra corresponding to $\mathcal{L}_{\text{int}}^5$ (SI), $\mathcal{L}_{\text{int}}^7$, $\mathcal{L}_{\text{int}}^{13}$, and $\mathcal{L}_{\text{int}}^{15}$ (SD) (two top panels), comparing these with the magnetic and electric dipole moment interactions of $\mathcal{L}_{\text{int}}^9$, $\mathcal{L}_{\text{int}}^{10}$, and $\mathcal{L}_{\text{int}}^{17}$ (bottom two panels). We set the interaction between the nucleon and WIMP at the weak scale, setting $d_i^p = d_i^n = 1$ for isoscalar and $d_i^p = -d_i^n = 1$ for isovector cases seprately, where as noted before we measure the couplings in units of the weak scale $1/m_V^2$, $m_V = 246.2$ GeV. The results are approximate accord with expectations. The SI interaction $\mathcal{L}_{\text{int}}^5$ should generate a scattering probability of relative size $(N \pm Z)^2$ for isoscalar or isovector couplings, coherent over the valence nucleons. For the magnetic and electric dipole interactions, we set $m_M = m_N$. Thus the nuclear scattering is governed by the familiar scattering off constituent nucleon magnetic moments, while the WIMP moments are governed by the same scale. This produces an operator hierarchy in powers of $(q/m_N)^2$, a scale that naturally arises in the nonrelativistic effective theory from a proper treatment of the relative velocity operator $\vec{v}^\perp$, as discussed in [11].

To constrain WIMP EFT couplings, we use two low-background physics runs of the PandaX-II experiment with a total exposure of 54-ton-days, Run 9 with 79.6 live days in 2016 and Run 10 with 77.1 live days in 2017. The S_1 and S_2 signal distributions from the standard SD and EFT models are obtained using the NEST model [22], which takes into account the PandaX-II detector parameters including the photon detection efficiency, electron extraction efficiency, single electron gain and the elec-
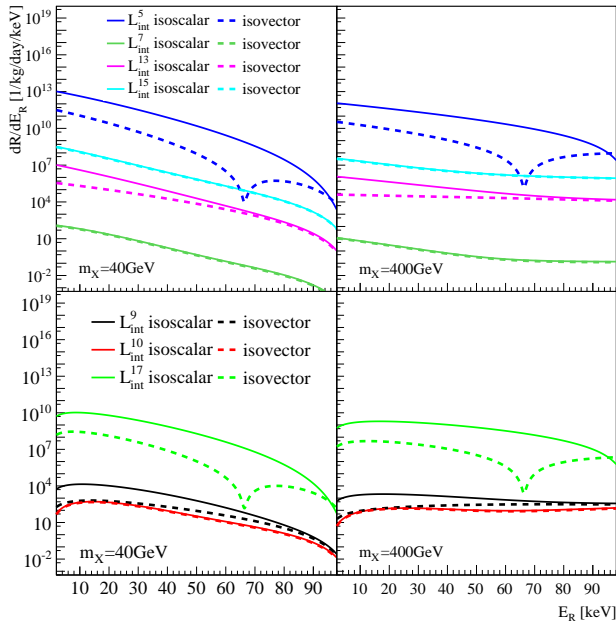
FIG. 1: Recoil energy spectra of EFT operators for spin-1/2 WIMPs on xenon nuclei. Top: dimension-four EFTs, including $\mathcal{L}_{int}^5$, $\mathcal{L}_{int}^7$, $\mathcal{L}_{int}^{13}$ and $\mathcal{L}_{int}^{15}$. Two WIMP masses 40 GeV/c^2 and 400 GeV/c^2 are chosen for illustration. Bottom: dimension-five and dimension-six EFTs, including $\mathcal{L}_{int}^9$, $\mathcal{L}_{int}^{10}$ and $\mathcal{L}_{int}^{17}$. Unit isoscalar and isovector couplings are assumed.
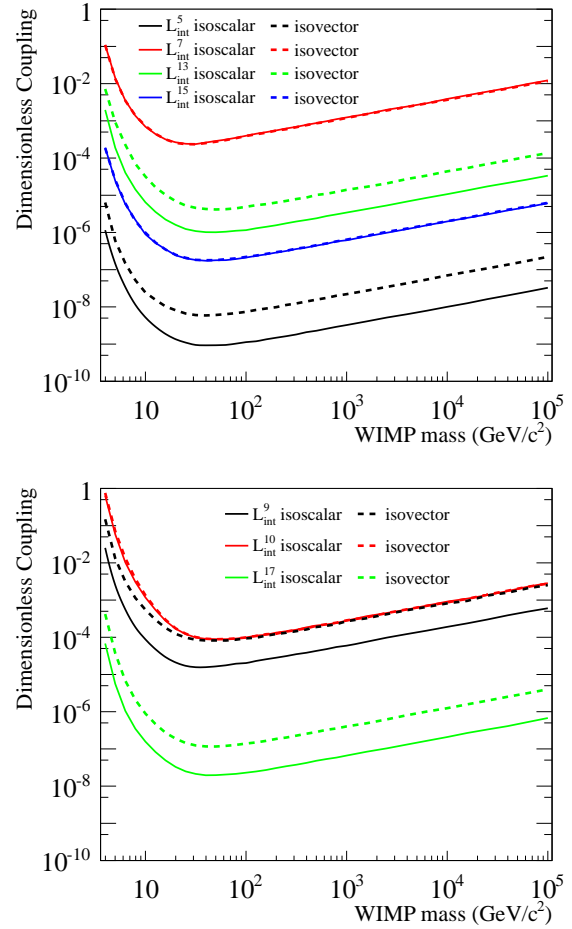

FIG. 2: The exclusion limits on the coefficients of relativistic EFT models. Top: dimension-four EFT models. Bottom: dimension-five and dimension-six EFT models.

tron lifetime. We adopt the same selection criteria as in Ref. [6]: events must have S_1 from 3 to 45 PE and S_2 from 100(raw) to 10000 PE, while also satisfying the quality cuts.

For heavy mass WIMPs and certain of the momentum-dependent EFT operators, a significant portion of the recoil energies E_R lie above ~ 40 keV. The current SI-oriented data selection is not fully optimized for such high recoil energies. It could be beneficial to extend the PandaX selection range for such operators, especially the S_1 cut. Such an analysis change is beyond the scope of this letter, but will be explored in future PandaX-II analyses.

In the current analysis, no significant deviation in Run 9 and Run 10 data sets is observed from the estimated background. For the EFT models, we calculated the upper limits on the WIMP-nucleon isoscalar and isovector couplings at 90% confidence level (C.L.) from the CL_{s+b} approach [23, 24], following the same procedure as in Ref. [6]. The results are shown in Fig. 2. Among the dimension-four EFT interactions, the strongest constraint is for the SI vector-vector interaction with an isoscalar coupling. The limit on the isovector coupling is weaker because the coherence is limited to the valence neutrons. The constraints on vector-axial vector interactions are approximately five orders of magnitude weaker than those obtained for the SI interaction, reflect-

ing the coherence of the latter and the WIMP-nucleon relative velocity dependence of the former, which generates a q^2/m_N^2 suppression in the rate. For higher dimension EFT interactions, the constraint on electric dipole moment term is much stronger than that on the magnetic dipole moment interaction.

We also placed constraints on the standard SD interaction for both neutron and proton couplings – equivalent to the relativistic interaction $\mathcal{L}_{int}^{15}$, or equivalently the nonrelativistic operators $\mathcal{O}_4$. As SD scattering requires a target $J_N > 0$, the participating isotopes are the odd-A xenon nuclei ^{129}Xe$(J = 1/2)$ and ^{131}Xe$(J = 3/2)$ with natural abundances of 26.4% and 21.2%, respectively. The 90% C.L. upper limits for the SD WIMP-nucleon cross sections are shown in Fig. 3. The lowest cross-section limits obtained are 9.0×10^{-42}cm^2 for WIMP-neutron only coupling and 2.2×10^{-38}cm^2 for WIMP-proton only coupling at a WIMP mass of 40 GeV/c^2. Results are given for both the standard SD interaction (red solid lines) and its chiral EFT analog (red dashed):
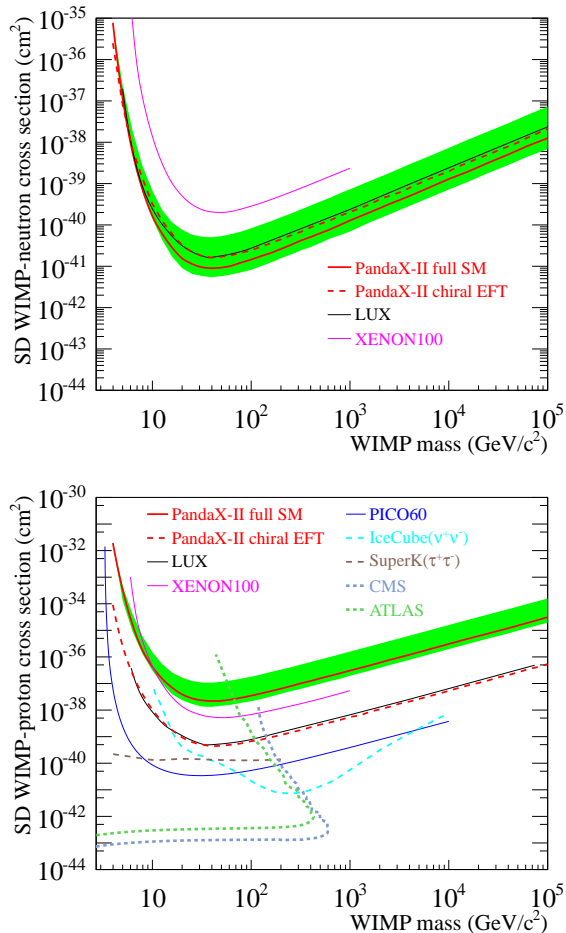
FIG. 3: The exclusion limits on the WIMP-nucleon cross section from the standard SD calculation. Top: neutron-only coupling. Bottom: proton-only coupling. Selected recent world results are plotted for comparison, including LUX [5], XENON100 [9], ATLAS [16], CMS [17], PICO-2L [25],PICO-60 [26, 27], IceCube [28] and Super-K [29]. The 1-σ bands are shown in green.

as discussed previously, as the odd isotopes of xenon have an unpaired neutron, the proton SD cross section is suppressed, leading to significant differences between the SD and chiral EFT exclusions in this case. The neutron limit is improved compared with existing best results [5].

In conclusion, we derive new limits on WIMP couplings for EFT interactions, using PandaX-II Run 9 and Run 10 data with an exposure of 54-ton-days. We have determined tightest constraints so far on a number of new interactions between WIMPs and nucleons. In addition, the most stringent upper limit to date on the SD WIMP-neutron cross section above WIMP mass of 40 GeV/c^2 is set, with a lowest excluded value of 9.0×10^{-42}cm^2 at a WIMP mass of 40 GeV/c^2. The minimum constraint on WIMP-proton cross section is 2.2×10^{-38}cm^2 at 90% confidence level at WIMP mass of 40 GeV/c^2.

* Spokesperson: xdji@sjtu.edu.cn
† Corresponding author: nzhou@sjtu.edu.cn
‡ Corresponding author: haxton@berkeley.edu

[1] J. L. Feng, Ann. Rev. Astro. Astrophys. **48**, 495 (2010).
[2] G. Bertone, D. Hooper, and J. Silk, Phys. Rep. **405**, 279 (2005).
[3] J. Liu, X. Chen, and X. Ji, Nature Phys **13**, 212 (2017).
[4] D. Akerib et al. (LUX Collaboration), Phys. Rev. Lett. **118**, 021303 (2017).
[5] D. S. Akerib et al. (LUX Collaboration), Phys. Rev. Lett. **118**, 251302 (2017).
[6] X. Cui et al. (PandaX-II Collaboration), Phys. Rev. Lett. **119**, 181302 (2017).
[7] C. Fu et al. (PandaX-II Collaboration), Phys. Rev. Lett. **118**, 071301 (2017).
[8] E. Aprile et al. (XENON Collaboration), Phys. Rev. Lett. **119**, 181301 (2017).
[9] E. Aprile et al. (XENON Collaboration), Phys. Rev. **D94**, 122001 (2016).
[10] E. Aprile et al. (XENON Collaboration), arXiv: 1805.12562 (2018).
[11] N. Anand, A. L. Fitzpatrick, and W. C. Haxton, Phys. Rev. C **89**, 065501 (2014).
[12] K. Schneck et al. (SuperCDMS Collaboration), Phys. Rev. **D91**, 092004 (2015).
[13] E. Aprile et al. (XENON Collaboration), Phys. Rev. **D96**, 042004 (2017).
[14] Z. Liu, Y. Su, Y. S. Tsai, B. Yu, and Q. Yuan, JHEP **11**, 024 (2017).
[15] J. Goodman, M. Ibe, A. Rajaraman, W. Shepherd, T. M. Tait, and H.-B. Yu, Phys. Rev. **D82**, 116010 (2010).
[16] M. Aabound et al. (ATLAS Collaboration), JHEP **01**, 126 (2018).
[17] A. M. Sirunyan et al. (CMS Collaboration), JHEP **07** (2017).

[18] J. Mendendez, A. Poves, E. Caurier, and F. Nowacki, Nucl. Phys. **A818**, 139 (2009).

[19] A. L. Fitzpatrick, W. C. Haxton, C. Johnson, and K. S. McElvain, in preparation for Ann. Rev. Nucl. Part. Sci. (2018).

[20] J. D. Lewin and P. F. Smith, Astropart. Phys. **6**, 87 (1996).

[21] P. Klos, J. Menendez, D. Gazit, and A. Schwenk, Phys. Rev. **D88**, 083516 (2013).

[22] B. Lenardo, K. Kazkaz, A. Manalaysay, J. Mock, M. Szydagis, and M. Tripathi, IEEE Trans. Nucl. Sci. **62**, 3387 (2015).

[23] A. L. Read, J. Phys. **G28**, 2693 (2002).

[24] T. Junk, Nucl. Instrum. Meth. **A434**, 435 (1999).

[25] C. Amole et al. (PICO Collaboration), Phys. Rev. **D93**, 061101 (2016).

[26] C. Amole et al. (PICO Collaboration), Phys. Rev. **D93**, 052014 (2016).

[27] C. Amole et al. (PICO Collaboration), Phys. Rev. Lett. **25**, 251301 (2017).

[28] M. G. Aartsen et al. (IceCube Collaboration), JCAP **04**, 022 (2016).

[29] K. Choi et al. (Super-Kamiokande Collaboration), Phys. Rev. Lett. **114**, 141301 (2015).